

## 3D-DLCS Reconstruction of Asymmetrically Undersampled Radial $^{23}\text{Na}$ -MRI

Nicolas G. R. Behl<sup>1</sup>, Christine Gnahn<sup>1</sup>, Peter Bachert<sup>1</sup>, and Armin M. Nagel<sup>1</sup>

<sup>1</sup>Medical Physics in Radiology, German Cancer Research Center (DKFZ), Heidelberg, Germany

**Target Audience:** Scientists and physicians interested in the field of non-proton MRI

### Purpose

Within the last years,  $^{23}\text{Na}$ -imaging has benefitted from several developments such as ultra-high field MR systems and optimized acquisition techniques. Nevertheless, the drawbacks of  $^{23}\text{Na}$ -MRI still are long acquisition times and low spatial resolutions<sup>1</sup>. The recent application of compressed sensing (CS) reconstruction algorithms has been shown to markedly improve SNR while reducing measurement times<sup>2,3,4,5</sup>. In this work we propose the use of an asymmetric 3D density adapted radial sampling pattern<sup>6</sup> that exploits the k-space symmetry, in combination with a 3D-Dictionary-Learning Compressed Sensing reconstruction (3D-DLCS)<sup>7</sup>.

### Methods

Simulated T2-weighted and measured in-vivo 3D-radial  $^{23}\text{Na}$ -MRI datasets were reconstructed with Nonuniform Fast Fourier Transform (NUFFT)<sup>8</sup> and 3D-DLCS. In both cases, one dataset was acquired using a uniform distribution of the projections and moderate undersampling (undersampling factor (USF) = 14.4). The other dataset was acquired with asymmetric undersampling in order to take advantage of the point symmetry of k-space. For the asymmetric undersampling, 60% of k-space were moderately undersampled (USF = 10) while for the remaining 40%, the undersampling factor was increased by a factor 4 (USF = 40). In both cases, the total number of projections was kept constant (6300). For the asymmetrically undersampled case, the missing projections were filled by interpolation from the measured projections<sup>9</sup> up to the Nyquist-limit for USF =

$40, k_{\max} = \sqrt{\frac{N_{\text{proj,nyq}}}{40 \cdot 4\pi}} / L$ .  $N_{\text{proj,nyq}}$  is the number of projections needed to fulfill the Nyquist criterion and L is the field of view. The remaining points beyond the Nyquist limit were zero-filled for the NUFFT reconstruction and left as free parameters for the 3D-DLCS reconstruction.

**Simulation:** The nominal resolution for the simulated data was  $\Delta x^3 = 1.7 \times 1.7 \times 1.7 \text{ mm}^3$ , TE/TR = 0.55/25ms. Five averages were simulated, leading to a total virtual measurement time  $T_{\text{AQ}} = 13.1 \text{ min}$ . The image quality of the 3D-DLCS reconstructions was assessed with the structural similarity index measure (SSIM) and peak-signal-to-noise ratio (PSNR).

**In-vivo data:** A healthy volunteer (female age 29) was measured on a 7 T whole body MR system (Magnetom 7 T, Siemens Healthcare, Erlangen, Germany). A double-resonant ( $^1\text{H}$ : 297.2 MHz;  $^{23}\text{Na}$ : 78.6 MHz) quadrature birdcage coil (Rapid Biomed GmbH, Rimpar, Germany) was used.  $\Delta x^3 = 1.7 \times 1.7 \times 1.7 \text{ mm}^3$ , TE/TR = 0.55/25ms,  $\alpha = 67^\circ$ , seven averages were acquired, the total measurement time was  $T_{\text{AQ}} = 18.4 \text{ min}$ .

### Results

The 3D-DLCS reconstruction of the uniformly undersampled simulated data shows artifacts that cannot be corrected by the iterative reconstruction. These appear as hypointense regions in fig. 1b that are not visible in the ground truth (fig. 2). These artifacts are not present in the reconstruction of the asymmetrically undersampled dataset (fig. 1d). This visual impression is confirmed by the increase of SSIM and PSNR shown in table 1. The reconstructions from the volunteer measurement presented in fig. 3 show similar results. While the strong undersampling in the uniform case makes it difficult to delineate small structures, these are better resolved with asymmetric undersampling. In both cases, noise-like artifacts are strongly reduced in the 3D-DLCS reconstruction compared to the NUFFT.

### Discussion & Conclusion

$^{23}\text{Na}$ -MRI was performed with an asymmetrically undersampled 3D-radial k-space trajectory in combination with a 3D-DLCS iterative reconstruction. The reconstructions of simulated data show reduced artifacts in the asymmetrically undersampled case. Reconstructions of in-vivo data display a better delineation of small structures and reduced blurring.

### References

- [1] Madelin & Regatte, J Magn Reson Imaging (2013) 38:511-29. [2] Lustig M et al., Magn Reson Med (2007) 6:1182-95. [3] Atkinson et al., Proc. Intl. Soc. Mag. Reson. Med. 16 (2008), p.335. [4] Madelin et al., J Magn Reson (2011) 214:360-365. [5] Gnahn et al., Magn Reson Med (2014) 5:1720-32. [6] Nagel et al., Magn Reson Med. 2009 62:1565-73. [7] Behl et al., In: Proc. ISMRM 22, p. 1524 (2014). [8] Fessler et al., Trans. Signal Process. (2003) 2:560-74 [9] Boada et al., Magn Reson Med (1997) 3:470-7.

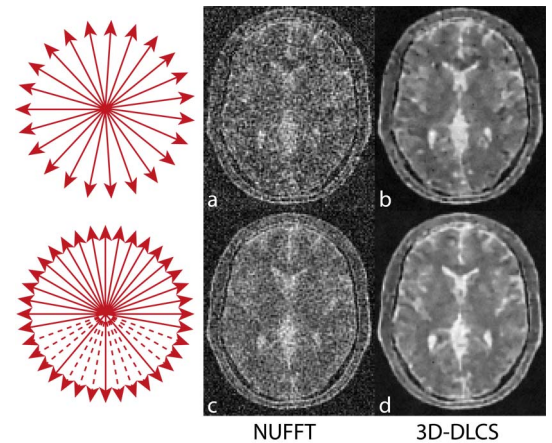


**Fig. 1:** Simulated data. (a-b): NUFFT and 3D-DLCS reconstructions with uniform undersampling (USF = 14.4); (c-d) reconstructions with asymmetric undersampling (USF<sub>1</sub>=10, USF<sub>2</sub>=40).

**Table 1:** PSNR and SSIM values for the 3D-DLCS reconstructions in fig. 1

|          | Uniform<br>(3D-DLCS) | Asymm.<br>(3D-DLCS) |
|----------|----------------------|---------------------|
| PSNR[dB] | 16.8                 | 17.9                |
| SSIM     | 0.44                 | 0.48                |

**Fig. 2:** Ground truth used for SSIM and PSNR calculation

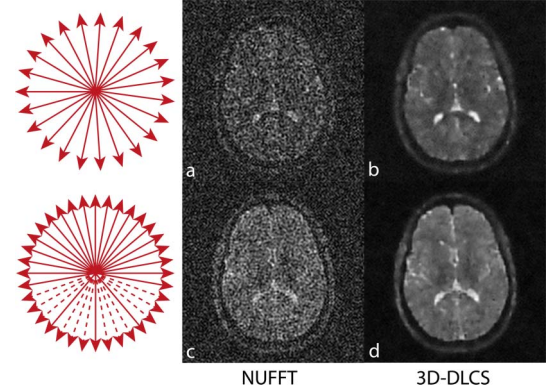
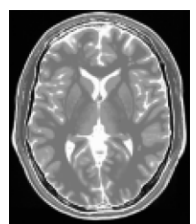


**Fig. 3:** In-vivo data. (a-b): NUFFT and 3D-DLCS reconstructions of in-vivo  $^{23}\text{Na}$ -data with uniform undersampling (USF = 14.4); (c-d) reconstructions with asymmetric undersampling (USF<sub>1</sub>=10, USF<sub>2</sub>=40).